Characterization of boria-alumina mixed oxides prepared by a sol-gel method. Part 1: NMR characterization of the xerogels

Franck Dumeignil, Michel Guelton, Monique Rigole, Jean Grimblot

Characterization of boria-alumina mixed oxides prepared by a sol-gel method.

Part 1: NMR characterization of the xerogels

Franck Dumeignil[a], Monique Rigole, Michel Guelton, Jean Grimblot*

Laboratoire de Catalyse de Lille, UMR CNRS 8010, Université des Sciences et Technologies de Lille, Bâtiment C3, 59655 Villeneuve d'Ascq CEDEX, France

[a] Present address: Department of Chemical Engineering, Tokyo University of Agriculture and Technology, 2-24-16 Nakacho, Koganei, Tokyo 184-8588, Japan

***** Author to whom correspondence should be addressed: jean.grimblot@ensc-lille.fr

Introduction of boron in the sol-gel preparation induces the creation of tetrahedral alumina species in the boehmite network initially exclusively constituted of octahedral aluminum species.

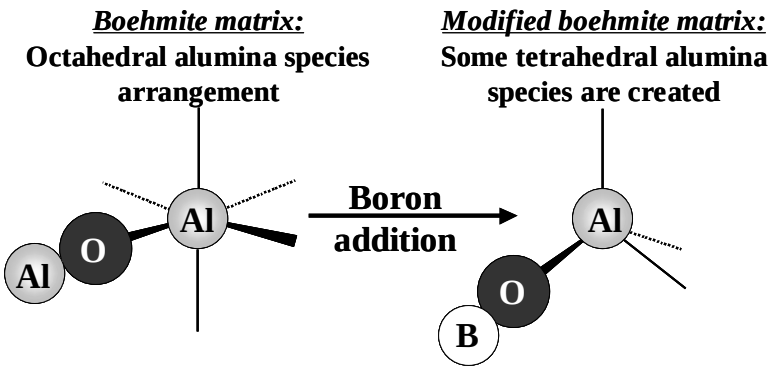

Keywords: sol-gel, alumina, boron, solid state MAS-NMR, structure

Abstract

While boria-alumina mixed oxides have been widely used for various catalytic reactions, their structure has never been satisfactory elucidated and is still a matter of debates. The present paper deals with the elucidation of the structure of boria-alumina prepared by a sol-gel method with B / Al atomic ratio varying from 0.013 to 1.643. The powders were prepared by hydrolysis of aluminum tri-sec-butoxide in presence of $(NH_4)_2B_4O_7.4H_2O$. Then, the solid-state magic angle spinning NMR spectroscopy was used to characterize the obtained solids in the dried state (xerogels), the calcined state being the object of a next paper. Both ^{27}Al and ^{11}B MAS-NMR spectra were recorded with subsequent simulation of these last ones. This allowed to build a consistent structural model of these xerogels, taking into account the evolutions of calculated parameters such as the quadrupolar interaction, the real chemical shift, the relative quantity of respectively BO_3, BO_4, tetrahedral, pentahedral and octahedral aluminum species as a function of the B / Al atomic ratio. As a result, it was found that for B / Al < 0.06, presence of boron induces the creation of bulk and surface tetrahedral aluminum species. Then, for B / Al > 0.06, BO_3 chains attached to these tetrahedral aluminum species are formed and start to grow through the matrix. Further, for B / Al > 0.15, when the boron loading increases, the BO_3 chains progressively emerge outside of the matrix, crossing it over. Furthermore, for B / Al > 0.26, some pentahedral aluminum species are formed supposedly due to the considerable steric strains afforded by some particular aluminum atoms. In brief, the presented model elucidates the structure of the dried alumina-based xerogels and is the key starting point to explain the structure of the oxides obtained after calcination and presented in the following paper.

Introduction

In the literature, numerous examples can be found for the use of boria-alumina mixed oxides for catalyzing various reactions. Firstly, such solids can be used directly as the active phase. This is the case for reactions such as the Beckmann rearrangement of cyclohexanone [1-8], the dehydration of alcohols such as methanol[9], isopropanol[10, 11] or butanol[12], the partial oxidation of alcanes such as ethane [13-16] or propane[17], cracking reactions [18-21], but-1-ene[22] and the m-xylene isomezation[8,23], and finally toluene disproportionation[23,24]. Boria-alumina mixed oxides can also be used for supporting active phases (typically metals). For instance, boria-alumina supported Re has been used for metathesis reactions[25, 26], supported Pt has been used for cyclohexene hydrogenation[27], n-heptane conversion, dehydrocyclisation[28] and hydroconversion[29] of n-octane. Supported Ru has been used for CO hydrogenation[30]. In contrast, while the use of boria-alumina supported hydrotreating catalysts is claimed in several patents [31-39], the literature describing them and / or their oxide precursors is rather scarce [40-52]. In fact, as a general matter, the B-Al_2O_3 system itself is not well described and the proposed interpretations concerning the solids structures are even sometimes contradictory. The present work is an extension of a study performed on a series of boria-alumina mixed oxides with low boron loadings[53]. We propose subsequent details of the previously proposed model for a wider range of boron loadings and the present paper deals specifically with the description of the structure of B-Al_2O_3 xerogels. The following paper will deal with the elucidation of the structure of these xerogels after calcination. The solids were prepared by a sol-gel synthesis method using a wide range of B / Al atomic ratios. Indeed, this method permits to obtain solids with high specific surface areas, and therefore a supposedly high dispersion of the B species within the alumina matrix, which might be interesting for catalytic applications such as the ones described above. The structure determination of the dried solids (xerogels) was mainly investigated by the solid-state magic

angle spinning nuclear magnetic resonance (MAS-NMR) spectroscopy. The use of a strong magnetic field permitted to obtain a rather good resolution of the spectra. However, the ^{11}B spectra shape and chemical shift were still disrupted by strong quadrupolar interactions. Therefore, the spectra were simulated using a specific software (QUASAR), which permitted to access to various parameters such as the quadrupolar interaction, the real chemical shift and the BO_4 / BO_3 ratio, as both species were detected on the prepared solids. The results were then thoroughly discussed and interpreted in order to build a consistent model of these xerogels. It was shown that their structure was strongly dependent of the boron loading and this dependency was substantially preserved after calcination as proved by the use of several methods of characterization (next paper[54]). This *sample memory* confirms *a posteriori* the validity of the model presented in the present paper.

Experimental section

Gel synthesis

The boria-alumina gels were synthesized according to an original sol-gel procedure described elsewhere. 150 cm^3 of butan-2-ol were placed under stirring at 85°C in a reflux apparatus together with the boron precursor [$(NH_4)_2B_4O_7.4H_2O$]. Then, after addition of 50 cm^3 of aluminum-tri-sec-butoxide [$Al(OC_4H_9)_3$ or ASB], the transparent solution became whitish due to partial hydrolysis of the alkoxide by the crystallization water of the boron salt. When the thermal equilibrium was reached, ASB was complexed with butan-1,3-diol with a molar ratio ASB / butan-1,3-diol = 2 (35 cm^3 of butan-1,3-diol). The hydrolysis step was then performed with 35 cm^3 of water (molar ratio H_2O / ASB = 10). Indeed, prehydrolysis by hydration water present in the boron salt may induce initial uncontrolled microstructure, but further, addition of butan-1,3-diol which complexes the Al alkoxide, permits to control the hydrolysis step. Such a

beneficial influence of a complexing agent has already been shown for preparation of pure alumina[55]. The obtained gel was kept under stirring at 85°C for 1 h and was then stored at room temperature for one hour. The gel containing the residual solvent was dried in a rotary evaporator under primary vacuum at 45°C. The obtained powder was then dried overnight at 100°C in an oven. As already reported elsewhere, the BET surface area of the xerogels are very high with a mean value at about 500 $m^2.g^{-1}$.

Sample compositions

Bulk atomic composition of the samples was determined at the *Service Central d'Analyses du CNRS* (Vernaison, France) by X fluorescence. For all the dried samples, the measured bulk composition was slightly equal to the expected one taking into account the relative amounts of B and Al precursors for gels preparation. This indicates that *(i)* there is not departure of volatile boron species (B_2O_3-like species) during the drying step, *(ii)* the preparation procedure is well controlled and *(iii)* the titration method gives correct results. Note that for the calcined mixed oxides, there is no more equality between measured and expected B-Al composition for high boron loading samples. Hereafter, the sample compositions will be reported as atomic B / Al ratio.

MAS-NMR spectroscopy

The MAS-NMR spectroscopy was used in order to characterize the local environment of the aluminum and the boron species in the dried xerogels. The spectra were recorded on a Brüker ASX 400 spectrometer working at 104.229 MHz (^{27}Al) and 128.33 MHz (^{11}B). The ^{27}Al spectra were recorded at a rotation frequency of 15000 Hz, with a pulse length of 0.8 μs and a repetition time between two acquisitions of 3 s; the reference at 0 ppm was taken for $Al(H_2O)_6^{3+}$. The ^{11}B spectra were recorded with a rotation frequency of 14500 Hz, with a pulse length of 10 μs and a repetition time of 10 s, the reference at 0 ppm being taken for $BF_3.OEt_2$.

Results

^{27}Al NMR

The ^{27}Al spectra of all the prepared samples are presented in Figure 1. Whatever the xerogel, the main detected signal in the 0-10 ppm range is assigned to octahedral aluminum species; such a species is classically detected on dried aluminas prepared by a sol-gel route[56]. At high boron loadings (B / Al > 0.263), the rise of another signal near 65 ppm can be clearly distinguished. It can be attributed to tetrahedral aluminum species[56, 57] . Focusing on this region of the corresponding spectra (Figure 2), an evolution of the chemical shift to the low frequencies (ppm) region of the peak attributed to the tetrahedral aluminum species can be observed when the boron loading increases. This chemical shift was accompanied by a visible increase in the relative proportion of this tetahedral aluminum species. Moreover, especially for high boron loadings, a peak that can be attributed to penta-coordinated aluminum species appeared near 30 ppm. Figure 3 presents the proportions of tetrahedral and penta-coordinated aluminum species obtained by direct integration of the respective peaks after classical peak decomposition. Clearly, four distinct domains can be observed. In domain I, from B / Al = 0 to B / Al ~ 0.05, the quantity of the tetrahedral aluminum species increases linearly with the B / Al ratio. Then, in domain II, between B / Al ~ 0.05 and B / Al ~ 0.14, this quantity remains constant. In domain III, between B / Al ~ 0.14 and B / Al ~ 0.47, the tetrahedral aluminum quantity increases again and the creation of penta-coordinated aluminum species starts for B / Al > 0.26. This penta-coordinated aluminum species will be later called « pentahedral aluminum species » for convenience, even if this denomination might not be really representative of the stereochemical conformation of such species. Further, Figure 4 presents the chemical shifts of the tetrahedral and the octahedral aluminum species for all the boron loadings, while Figure 5 focuses on low boron loadings. Again, the same four domains can be distinguished. In domain I, the chemical shifts of

tetrahedral and octahedral aluminum species peaks are constant, despite a slightly high value for B / Al = 0 in the case of the octahedral species. The values for the octahedral species can nevertheless be reasonably considered as constant, taking into account the experimental error on the chemical shift determination reported in Figure 5. In domain II, the chemical shifts of the peaks due to tetrahedral and octahedral aluminum species start to decrease linearly with the B / Al atomic ratio. Then, while the decrease in the chemical shift of the octahedral aluminum species peak goes on to vary linearly in domain III, the one of the tetrahedral aluminum species becomes less marked. Finally, in domain IV, the octahedral aluminum species chemical shift seems to stabilize while in the same time the slight decrease in the tetrahedral aluminum species chemical shift previously observed goes on.

^{11}B-NMR

Figure 6 shows that the boron signal comprises two features up to B / Al = 0.138 (domains I and II). The feature observed at high frequencies (ppm) is due to the trigonal boron species, hereafter called BO_3 species. The peak shape is affected by a strong second order quadrupolar interaction [58-64]. This quadrupolar interaction is responsible for a signal splitting that induces an experimental broadening for the conditions of this study and additionally shifts the peak to the lower ppm region. Then, the rather narrow peak observed near 0 ppm, superposed to the one assigned to the BO_3 species, is due to the presence of tetrahedral boron species, hereafter called BO_4 [65,66] species. The BO_4 species quantity seems to decrease when the boron loading increases up to B / Al = 0.138 (domains I and II). Moreover, for B / Al > 0.138, a third signal appears in the valley between the signals of trigonal and tetragonal boron species. This signal is likely to be due to as small quantity unreacted / decomposed / disrupted boron precursor remaining trapped in the dried xerogel. Further, for B / Al > 0.263, the signal due to the BO_4 species increases again with increasing the boron loading.

Due to the above-mentioned strong quadrupolar interaction, the interpretation of the boron spectra evolution from the direct visual observation is difficult. Therefore, the relative proportions of the B-oxygen containing species were determined using the QUASAR[67] spectrum simulation software. Indeed, this software permits to quantify the quadrupolar interaction and to recalculate the spectra that would have been obtained if no quadrupolar interaction modifies the signal. Consequently, this makes the results easier to interpret with a possible determination of the "true" chemical shift of each species and subsequently this permits reliable quantification that would make no sense to perform on the non-simulated spectra. Various parameters were taken into account to perform the simulations. Indeed, it is necessary to input an estimation of the true chemical shift, of the quadrupolar interaction, of the asymmetry of this interaction that contributes to modify the shape of the peaks, of the broadening of the peaks as well as some parameters induced by the spectrometer itself such as the rotation speed, the response factor or the dead time of the spectrometer. After manual adjustment of these parameters, the computer simulation is finely performed with a simplex algorithm. This algorithm permits to further fit the simulated spectrum by minimizing the difference with the experimental ones. During this calculation process, the computer adjusts the parameters initially inputted in a chemically acceptable range as imposed by the user.

Figure 7 shows that the calculated chemical shift of the BO_3 species peak (about 16 ppm) is greater than the one directly observed (about 10 ppm), due to a relatively high quadrupolar interaction near 2.25 MHz (Figure 8). For the BO_4 species, as the quadrupolar interaction is lower (between 0.3 and 0.85 MHz (Figure 8)), the observed chemical shift is quite close to the calculated ones, with a value near 2 ppm (Figure 7). As a remark, unlike in the case of the BO_3 species, the quadrupolar interaction on the BO_4 species is clearly affected by the boron quantity. Indeed, after an increase in the domain I, it becomes constant at about 0.85 MHz.

Discussion

The discussion is divided into two main parts: the first one is dealing with the low boron loading gels while the second one concerns high boron loading samples. Then, a global synthetic model will be proposed and commented.

Low boron loading samples (domains I and II)

Domain I

In a previous work, it was proposed that the tetrahedral aluminum species observed in domain I are generated concomitantly with the creation of the Al-O-B bonds, giving $Al_{tetra}(OAl)_{4-x}(OB)_x$ (x = 1 to 4) species. Indeed, in the absence of boron, tetrahedral aluminum species are hardly detected (Figure 2), meaning that their creation is indubitably linked to the presence of boron in the oxide system. Then, at the end of domain I (for B / Al > 0.05), a stabilization of the tetrahedral aluminum species quantity is observed, which represents then approximately 1 % of the total aluminum species. This value of 1 % corresponds almost to four boron atoms for one tetrahedraly coordinated aluminum atom. This is an indication that the tetrahedral aluminum species are progressively decorated with 1, 2, 3 and finally 4 boron species through Al-O-B bridges (for B / Al = 0.05). One would expect that this local structure is more likely induced by the rate of hydrolysis rather than by thermodynamic equilibrium. In domain I, the amount of B relative to Al is very weak so that the amount of water brought by the boron salt is weak and therefore uncontrolled hydrolysis of weak importance. Then the local structure of Al species is mainly controlled by hydrolysis of the diol-complexed Al alkoxide.

The nature of the boron species decorating the $Al_{tetra}(OB)_4$ species that will be later called “saturated” tetrahedral aluminum species has now to be clarified. As a preliminary remark, it is now well known that the BO_4 species in / on boria-alumina mixed oxides are created by a reversible hydration-dehydration reaction of BO_3 species, the NMR signal attributed to the BO_4

species disappearing completely after drying the solids. In addition, the existence of such a process was also demonstrated by thermogravimetry analysis by Cucinieri-Colorio *et al.*. Therefore, a BO_3 species can reversibly transform into a BO_4 species provided that this species is situated near the surface of the solid. Indeed, only the BO_3 entities on the surface of the solids can be presumably in contact with the water molecules present in ambient atmosphere. Thus, it can be deduced that the observed BO_4 species are surface species. Moreover, the increase in the quadrupolar interaction on the BO_4 species observed in domain I (Figure 8) can be easily explained. Indeed, while the presence of only one BO_4 species with one tetrahedral aluminum species may not induce a large strain on the involved species, the presence of a second BO_4 species linked to the same tetrahedral aluminum species might be responsible for an increase in the local steric hindrance. Indeed, in order to permit the second hydration of a BO_3 species, the host tetrahedral aluminum and well as the previously linked BO_4 must bear a distortion that is revealed by the increase in the quadrupolar interaction. From geometrical considerations, two BO_4 species bound to one tetrahedral aluminum species seems to be an acceptable maximum. In other words, it is supposed that the saturated surface tetrahedral aluminum species are rather likely to be anchored in the solid by two BO_3 species on one side, while two BO_4 species on the other side are emerging out of the solid surface. Then, the quadrupolar interaction for a single BO_4 species (i.e. one BO_4 species without constraint imposed by another BO_4 species) can be determined by extrapolating the curve giving the quadrupolar interaction of BO_4 species (Figure 8) to B / Al = 0. The obtained value is about 0.4 MHz. In Figure 8, it can be seen that this interaction increases with the addition of boron, up to the end of domain I (~ 0.8 MHz). This reflects the progressive creation of the tetrahedral aluminum species linked with one BO_4 and then with two BO_4 species. In other words, the increase observed in Figure 8 is due to a weighted average between the quadrupolar interaction of the ‘isolated’ BO_4 species (i.e. BO_4 species

bound to one tetrahedral aluminum species that is not linked with a second BO_4 species), and the one of the BO_4 species with another BO_4 species in its vicinity, attached to the same aluminum tetrahedral species. Then, the stabilization of the quadrupolar interaction value at the end of domain I reflects the fact that all the surface tetrahedral aluminum species are linked with two BO_4 species, these latter exhibiting all a comparable quadrupolar interaction. In addition, at the end of domain I, there are roughly 6 BO_3 species for 1 BO_4 species as $15 / 85 \cong 1 / 6$ (see Figure 9). Considering now all the previous observations concerning domain I, in particular that there are about 4 B atoms for 1 tetrahedral Al atom at the limit or i.e. 100 B atoms for 25 tetrahedral Al atoms, among these 100 B atoms, 15 are BO_4 species bound to an average value of 7.5 surface tetrahedral aluminum species. It is therefore expected that the tetrahedral aluminum species distribution within the mixed oxide at the domain I limit is 30 % at the surface (7.5 / 25 = 0.3) and 70 % inside (bulk) the matrix.

As a preliminary conclusion, all these results are consistent with the presence of various entities in domain I:

- $Al_{tetra}(OAl)_{4-x}(BO_3OH)_y(BO_3)_z$ (x = y + z, and y and z being equal or inferior to 2) species are present on the surface and $Al_{tetra}(OAl)_{4-w}(BO_3)_w$ (w between 1 and 4) species are located in the matrix.
- At the end of domain I, concerning tetrahedral aluminum species, there are about 70 % of $Al_{tetra}(BO_3)_4$ bulk sites and about 30 % of $Al_{tetra}(BO_3OH)_2(BO_3)_2$ surface sites.

Domain II

In domain II, the BO_3 species are largely predominant among the boron species (Figure 9). The BO_4 species proportion decreases when the boron loading increases suggesting that the introduced boron starts to form BO_3 chains, which is a general tendency of this element in the oxide form (e.g. the structure of B_2O_3). Then, in domain II, the linear decrease in the chemical

shift of the tetrahedral aluminum species (Figure 5) is probably due to the fact that this latter is influenced by the development of BO_3 ribbons (classical chain effect modulating finely the NMR chemical shift). In addition, it seems reasonable to postulate that the polymerization of the BO_3 ribbons is likely to take place on the boron species linked to the tetrahedral aluminum species previously "saturated" with four boron atoms [$Al_{tetra}(BO_3OH)_2(BO_3)_2$ or $Al_{tetra}(BO_3)_4$] as nucleation points.

As a partial conclusion, we suppose that two families of species can coexist in domain II, the $Al_{tetra}(BO_3)_m(BO_3)_n(BO_3)_o(BO_3)_p$ species and the $Al_{tetra}[BO_3OH(BO_3)_{m'}][BO_3OH(BO_3)_{n'}](BO_3)_{o'}(BO_3)_{p'}$ (m, n, o, p and m', n', o' p' indicating the chain lengths respectively).

In brief, for the xerogels with low boron loading:

- Boron introduction induces the creation of Al-O-B bonds leading to the creation of tetrahedral aluminum species in domain I;
- The tetrahedral aluminum species proportion reaches a maximum at the end of domain I and then stabilizes;
- Assuming that the formed surface tetrahedral aluminum species can be linked to a maximum of two BO_4, it is possible to propose a model describing the structure of the solids, which is consistent with the NMR observations;
- When the tetrahedral aluminum species are "saturated" by 4 surroundings boron atoms, i.e. 2 BO_3 and 2 BO_4 in the case of the surface species and 4 BO_3 in the case of the matrix species, BO_3 ribbons start to develop.

High boron loading samples (domains III and IV)

While the quadrupolar interaction remains constant for the BO_4 species for the high boron loadings (B / Al > ~ 0.15 in Figure 10), in domain III the quadrupolar interaction observed for

the BO_3 species slightly increases. Further, domain III corresponds to the creation of new tetrahedral species (Figure 3), which are exhibiting quite the same chemical shift as that of the saturated tetrahedral aluminum species (at the end of domain II in Figure 4). Therefore, since the chemical shift of the new species is the same, the nature of these newly created tetrahedral aluminum species is supposed to be likely the same as the one of the saturated species created for the ratio $B / Al \cong 0.15$. In addition, it was supposed previously that the BO_3 chain length influences the chemical shift of the tetrahedral aluminum species on which they are attached and Figure 4 shows that the chemical shift of the tetrahedral species in domains III and IV does not vary significantly. That means that the newly created tetrahedral aluminum species are linked to chains with a mean length equal to the one of the chains linked to the tetrahedral aluminum species present at the end of the domain II, as the chemical shifts of both species are almost equivalent. Moreover, for moderate boron loadings, there might be a limit in the length of the BO_3 chains, physically imposed by the thickness of the boehmite layer. All these observations are consistent if it is assumed that the new tetrahedral aluminum species are attached to the same chains as those issued from the initially created tetrahedral aluminum species (in domain I), i.e. if a new surface tetrahedral aluminum species is created at the end of an existing BO_3 chain emerging from a previously created tetrahedral aluminum species. In other words, the BO_3 ribbons cross over the alumina matrix to emerge on the other side, creating new surface aluminum tetrahedral species, themselves at the origin of new BO_3 chains subsequently developing through the alumina matrix when the boron loading increases. Thus, the BO_4 percentage, which constantly decreased in domains I and II because of the exclusive development of BO_3 chains, stabilizes due to the concomitant creation of BO_3 and new BO_4 species in domains III and IV (Figure 11). Further, as previously mentioned, it is found that the

quantity of tetrahedral aluminum species formed at the end of domain I is about 1 %. In addition, it is reasonable to suppose that each tetrahedral aluminum species can be the starting point of four BO_3 chains that can further generate four new tetrahedral aluminum species when crossing the matrix. If it this supposition is exact, one must obtain at maximum 5 % of tetrahedral aluminum species after all the BO_3 chains have emerged out. In fact, if the percentages of tetrahedral and pentahedral aluminum species created at the end of domain III are added, a value of about 4,5 % is obtained, which is in very good agreement with the formulated hypothesis. Now, it is supposed that the pentahedral aluminum species are created by an extreme distortion of particular tetrahedral aluminum species. Indeed, the quadrupolar interaction on the BO_3 species increases when the ratio B / Al = 0.15 is reached. This is supposedly due to the creation of BO_3 chains possessing at each extremity a surface tetrahedral aluminum species linked to two hydrated BO_3 species (BO_4). This involves strong steric constraints on each side of the chain. Indeed, the involved chains must satisfy two conformation exigencies on each extremity, increasing their torsion, which is reflected by an increase in the observed quadrupolar interaction. Therefore, some surface aluminum species must afford an extensive constraint, giving the formation of pentahedral aluminum species.

As a remark, the true chemical shifts of the BO_3 and BO_4 species in domains III and IV are not significantly affected because the chemical nature of these newly created species is not very different from that present in domains I and II.

Description of the proposed model

The results of the NMR study presented in this paper on boria-alumina mixed xerogel oxides combined with their discussion allows to propose a model (Figure 13), which is aiming to describe the evolution of the local structure of the boron and aluminum oxo-species in such solids when the relative amount of boron is increasing.

Without boron in the sample, the aluminum local structure is quite exclusively octahedral (see Figure 1 & Figure 2).

For low boron loadings (B / Al < 0.15), the solids exhibit an intermediate structure that we called induction phase of the system (Figure 13 (a), (b) and (c)):

- For B / Al < 0.06 (Figure 13 (a)), surface BO_4 species are created. Their formation induces the creation of surface tetrahedral aluminum species. BO_3 species are also present in the alumina matrix and their presence induces the creation of matrix tetrahedral aluminum species. Then, the surface tetrahedral aluminum species are progressively linked to two BO_4 and two BO_3 species, while the matrix tetrahedral aluminum species are progressively surrounded with 4 BO_3 species (Figure 13 (b and c));

- Then, for 0.06 < B / Al < 0.15 (Figure 13 (c)), the BO_3 and BO_4 species linked to the both surface and bulk tetrahedral aluminum species saturated with four boron oxo-species are the starting point for the development of BO_3 chains.

After this induction phase, the final system is forming for B / Al > 0.26 (Figure 13 (d) and (e)):

- For 0.15 < B / Al < 0.26 (Figure 13 (d)), the BO_3 chains are crossing over the alumina matrix and terminal BO_4 are created at the emerging point. The creation of the terminal BO_4 species is accompanied with the creation of new surface tetrahedral aluminum species.

- For B / Al > 0.26 (Figure 13 (e)), pentahedral aluminum species are created. They result from the distorsion of aluminum species that are particularly strained. Indeed, some surface tetrahedral aluminum species must afford extreme constraints due to the presence of not only two BO_4 species attached to them but also to the double distortion of one ore more BO_3 chain(s).

Comments and exploitation of the model

As a preliminary remark, it is possible to calculate the mean thickness τ of a sheet of matrix, from the value of the density ρ of the boehmite (about 3 $g.cm^{-3}$) and the average specific surface S of the xerogels for a low boron loading (~ 500 $m^2.g^{-1}$). The formula $\tau = 2 / \rho.S$ gives an average thickness of about 13 Å.

When the BO_3 chains emerge outside the matrix (in domain III), the creation of new surface tetrahedral aluminum species is induced. This sheet of 13 Å can be crossed by different ways because the BO_3 chains can supposedly develop spatially at random in all the directions. The chains that develop 'perpendicularly' to the layer are likely to be the ones that will emerge first. If the probability of development of each chain is supposed to be the same, i.e. the length of all the chains is the same, the progressive apparition of the new tetrahedral aluminum species in domain III corresponds to the random angular distribution of the BO_3 chains. Indeed, the more the direction of a chain deviates from a line perpendicular to the surface of the boehmite layer, the more the chain must be long to emerge on the other side of the surface. It is important to note that this notion of "perpendicularity" is just indicative assuming the fractal character of the solids. In addition, it is obvious that the chains emerging at first are the chains issued from the matrix tetrahedral aluminum species rather than the chains attached to the surface tetrahedral aluminum species, the length of the distance to cross being shorter (Figure 13 (d)). It is then interesting to note that pentahedral aluminum species are starting to be created only in the middle of domain III (Figure 3) for B / Al = 0.26. Indeed, it was supposed that they are created by an extreme distortion of BO_3 chains, which might happen for the chains that are issued from one side of a boehmite sheet and cross over the matrix to emerge on this other side.

In brief, the proposed structural model of the xerogels is consistent with all the NMR observations. The following paper will show that the results presented here fit very well with the

results obtained on the corresponding calcined solids by a combined set of characterization techniques such as solid-state NMR, XPS, XRD, etc. It is quite clear that the xerogel genesis has a noticeable influence on the final structure of boria-alumina mixed oxides with different B / Al atomic ratios.

Conclusions

In this first paper, boria-alumina prepared by a sol-gel method using various B / Al ratios have been characterized before further calcination by ^{27}Al and ^{11}B MAS-NMR spectroscopy. The spectra have been simulated in order to access to important parameters such as the effective BO_3 / BO_4 ratio and the quadrupolar interaction frequency. The features of the spectra as well as the calculated parameters evolves clearly with the B / Al atomic ratio. All the results are consistent with the presence of four distinct domains corresponding to four different structures that the system can exhibit according to the boron loading. In domain I ($B / Al < 0.06$), the introduction of B atoms induces the creation of tetrahedral aluminum species progressively surrounded with 4 boron oxo-species. At the end of domain I, 1 % of the aluminum species have a tetrahedral structure, the remainder being octahedral aluminum species like in the mother boehmite structure. In domain II ($0.06 < B / Al < 0.15$), the tetrahedral aluminum species locally saturated with boron oxo-species are the starting points of BO_3 chains growing at random in all the directions inside the host alumina matrix. In domain III ($0.15 < B / Al < 0.26$) the BO_3 chains are long enough to cross over the alumina matrix and emerge progressively. In addition, new surface tetrahedral aluminum species are created at the emergence point. These new aluminum species are then themselves the nucleation point of new BO_3 chains that develop for higher boron loadings. Furthermore, in this domain III, the mother alumina matrix is so stericaly disrupted that pentahedral aluminum species are formed to supposedly release the strains in the new material

network. Then, we can mention domain IV that corresponds to solids with high amount in boron (B / Al ~ 0.5 and more) and is only briefly mentioned for information as it progressively looses the boehmite character to transform into boria doped with Al. Finally, the NMR results have permitted to build a model of the boria-alumina xerogels. This model was not only of course consistent with the NMR observations but also with the results obtained on the same solids after calcination (following paper) where the existence of 4 domains is again demonstrated.

Acknowledgements

The authors would like to thank the European Community which have funded this work through the Joule III project n° JOF3-CT95-0002.

Figures captions

Figure 1. ^{27}Al NMR spectra of the xerogels with different amounts of boron.

Figure 2. Focus on the 20 - 85 ppm region of the ^{27}Al NMR spectra of the xerogels.

Figure 3. Proportion of tetrahedral and pentahedral aluminium species determined from the ^{27}Al NMR spectra.

Figure 4. ^{27}Al NMR chemical shifts of the octahedral and tetrahedral aluminum species.

Figure 5. ^{27}Al NMR chemical shifts of the octahedral and tetrahedral aluminum species (low boron loadings).

Figure 6. ^{11}B NMR spectra of the xerogels with different amounts of boron.

Figure 7. Observed and simulated chemical shifts of the peaks due to the boron oxo-species (low boron loadings).

Figure 8. Quadrupolar interaction frequency on the boron oxo-species (low boron loadings).

Figure 9. $\%BO_4$ defined as $\{B(BO_4)\} / [B(BO_4) + B(BO_3)]\} \times 100$ on calcined solids determined by QUASAR simulation (low boron loadings).

Figure 10. Quadrupolar interaction frequency on the boron species (full range of boron loadings)

Figure 11. $\%BO_4$ defined as $\{B(BO_4)\} / [B(BO_4) + B(BO_3)]\} \times 100$ on calcined solids determined by QUASAR simulation (full range of boron loadings).

Figure 12. Observed and simulated chemical shifts of the boron species (full range of boron loadings).

Figure 13. Proposed schematic model for the structure of the boria-alumina xerogels;

(a) Creation of tetrahedral aluminum species from Al-O-B bonds;

(b) Double hydration of boron species linked to tetrahedral aluminum species;

(c) Development of BO_3 chains;

(d) Emergence of BO_3 chains with creation of terminal BO_4 species inducing creation of new tetrahedral aluminum species;

(e) System evolution, creation of pentahedral aluminum species.

(✚) = tetrahedral aluminum species; (⬟) = pentahedral aluminum species; (▽) = BO_3 species; (□) = BO_4 species.

Figures

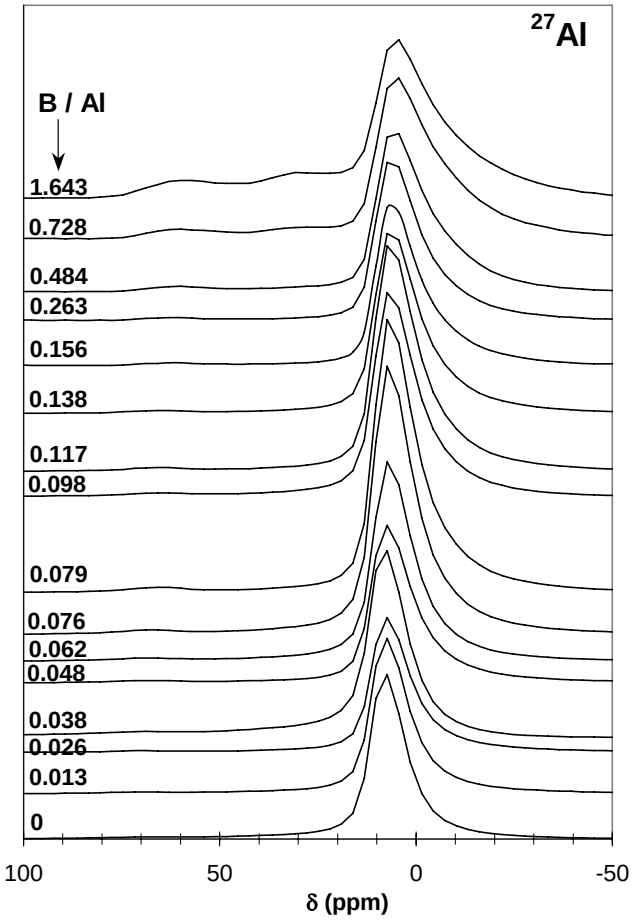

(Fig. 1)

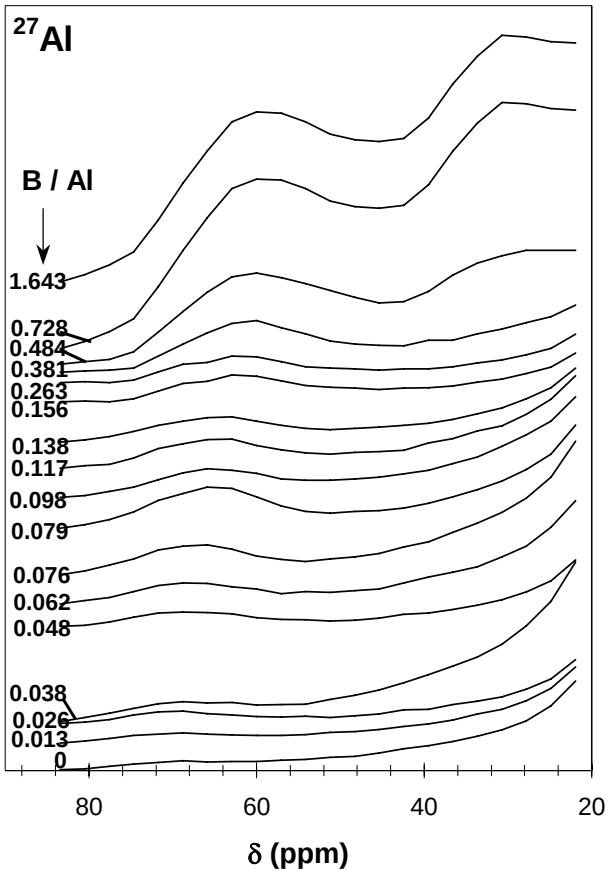
27Al
B / Al
1.643
0.728
0.484
0.381
0.263
0.156
0.138
0.117
0.098
0.079
0.076
0.062
0.048
0.038
0.026
0.013
0
80
60
40
20
δ (ppm)

(Fig. 2)

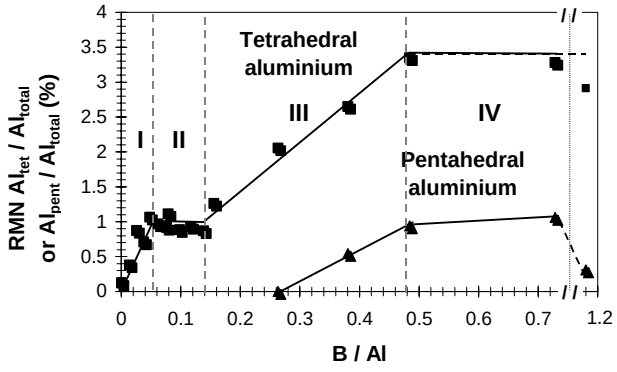
RMN Al_tet / Al_total
or Al_pent / Al_total (%)
Tetrahedral
aluminium
Pentahedral
aluminium
I
II
III
IV
0
0.5
1
1.5
2
2.5
3
3.5
4
0
0.1
0.2
0.3
0.4
0.5
0.6
0.7
1.2
B / Al

(Fig. 3)

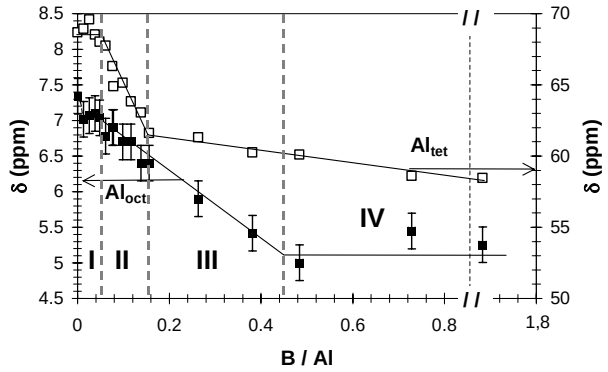
δ (ppm)
δ (ppm)
B / Al
Al_tet
Al_oct
I
II
III
IV

(Fig. 4)

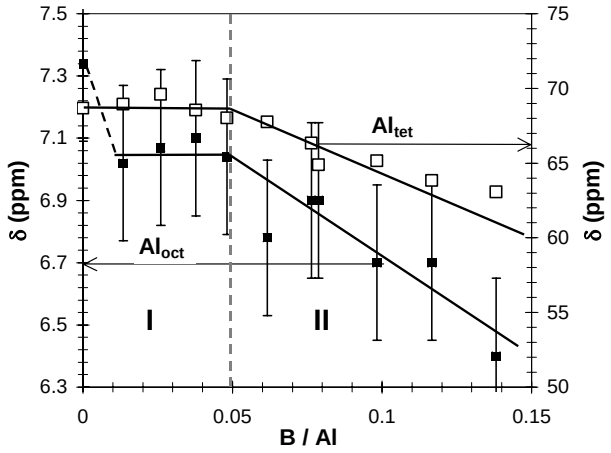
δ (ppm)
δ (ppm)
B / Al
Al_tet
Al_oct
I
II

(Fig. 5)

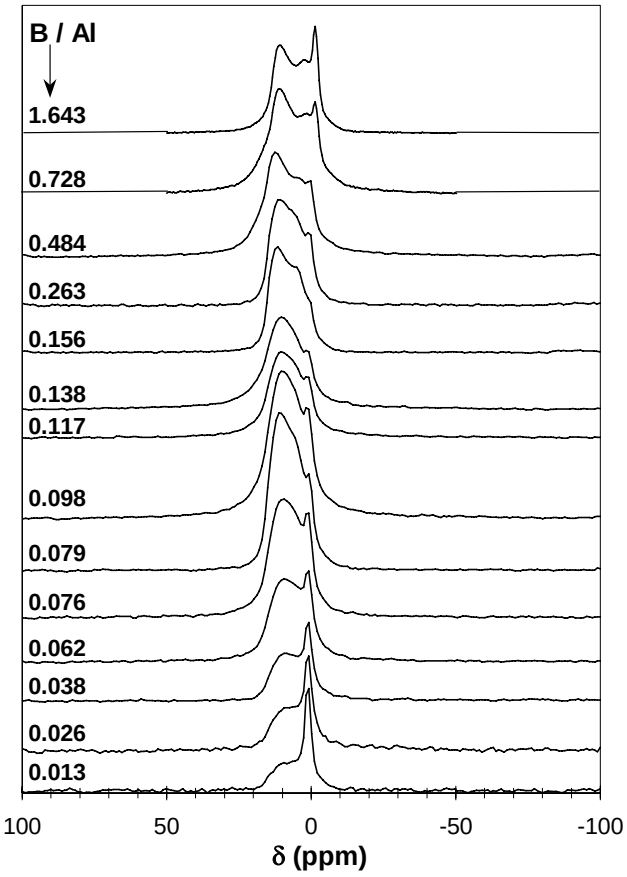
B / Al
1.643
0.728
0.484
0.263
0.156
0.138
0.117
0.098
0.079
0.076
0.062
0.038
0.026
0.013
100
50
0
-50
-100
δ (ppm)

(Fig. 6)

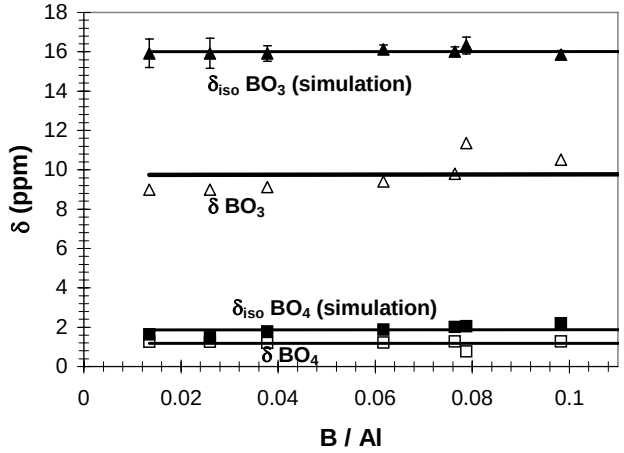
δ (ppm)
B / Al
δiso BO3 (simulation)
δ BO3
δiso BO4 (simulation)
δ BO4
0
2
4
6
8
10
12
14
16
18
0
0.02
0.04
0.06
0.08
0.1

(Fig. 7)

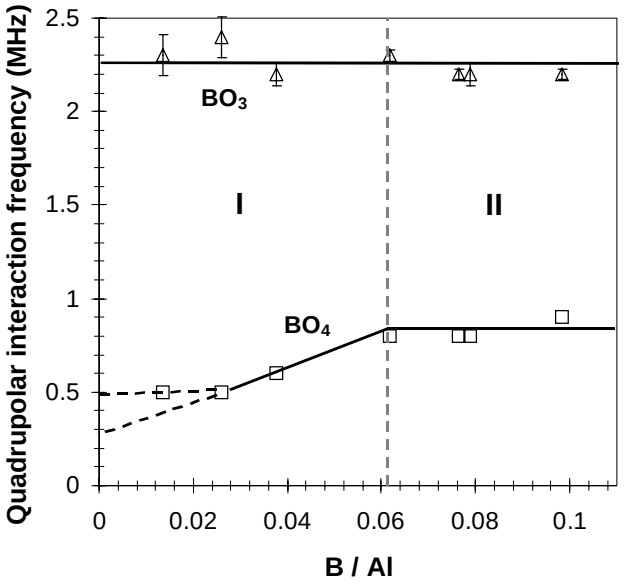

(Fig. 8)

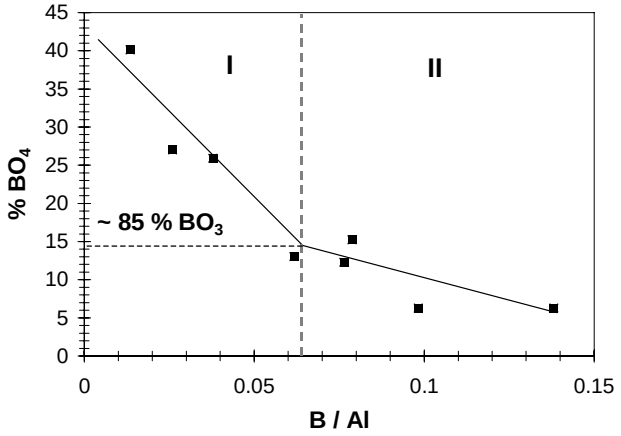

(Fig. 9)

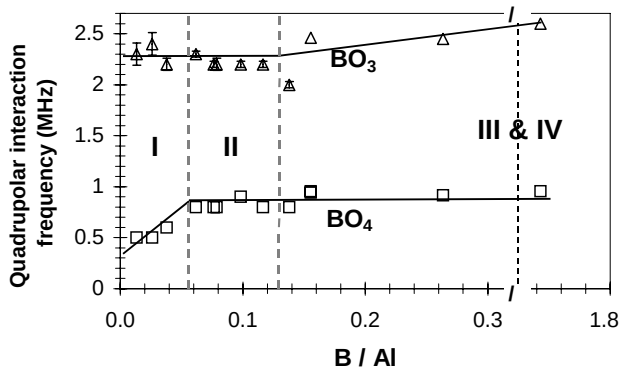

(Fig. 10)

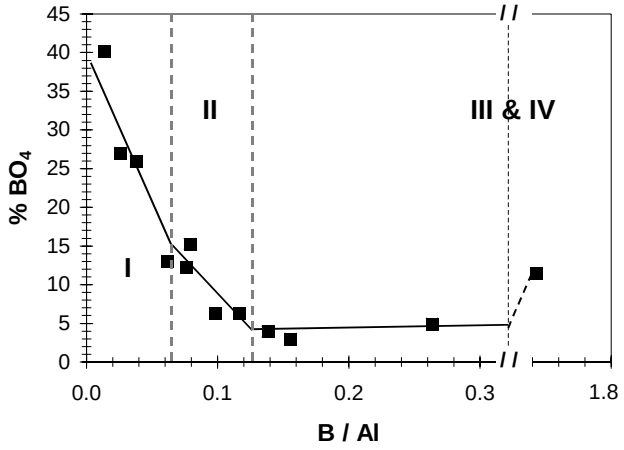
% BO4
B / Al
I
II
III & IV

(Fig. 11)

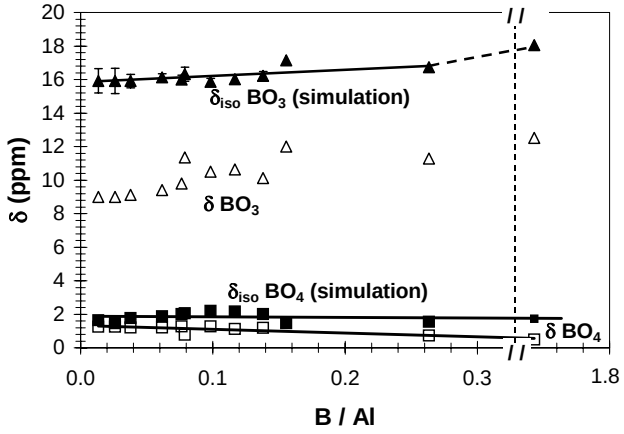
δ (ppm)
B / Al
δiso BO3 (simulation)
δ BO3
δiso BO4 (simulation)
δ BO4

(Fig. 12)

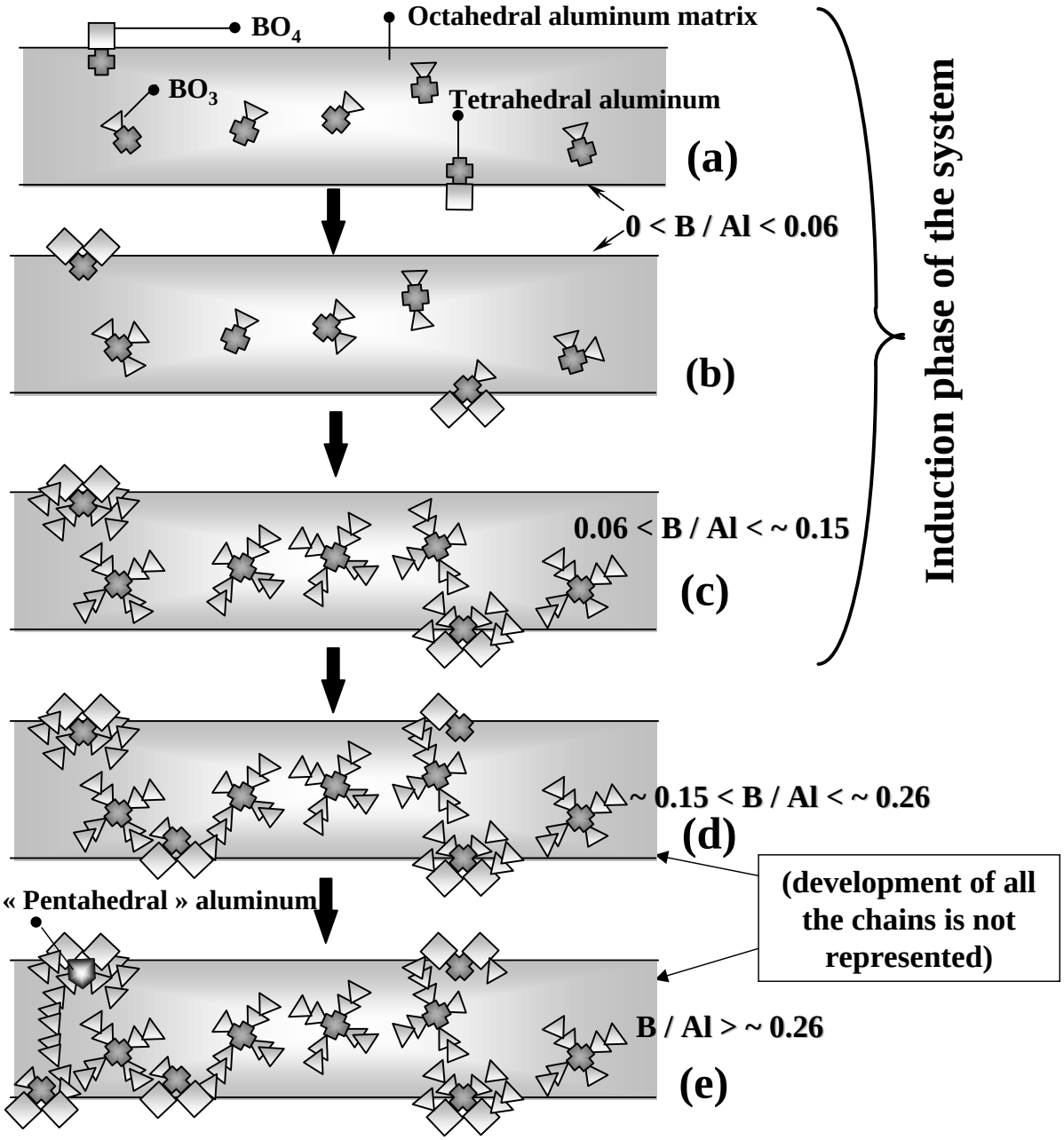
BO4
Octahedral aluminum matrix
BO3
Tetrahedral aluminum
(a)
0 < B / Al < 0.06
(b)
0.06 < B / Al < ~ 0.15
(c)
Induction phase of the system
~ 0.15 < B / Al < ~ 0.26
(d)
« Pentahedral » aluminum
(development of all the chains is not represented)
B / Al > ~ 0.26
(e)

(Fig. 13)

References

(1) Curtin, T.; McMonagle, J. B.; Hodnett, B. K. *Appl. Catal. A: Gen.* **1992**, *93*, 91.

(2) Izumi, Y.; Sato, S.; Urabe, K. *Chem. Lett.* **1983**, 1649.

(3) Curtin, T.; McMonagle, J. B.; Hodnett, B. K. *Appl. Catal. A: Gen.* **1992**, *93*, 75.

(4) Werke, L. *East Ger. Patent* 10920, 1955.

(5) Irnich, R., BASF, *Ger. Patent* 1227028, 1976.

(6) Immel, O. *et al.*, Bayer, *Jap. Patent* S53-037686, 1978.

(7) Murakami, Y.; Saeki, Y.; Ito, K. *Nippon Kagakukaishi* **1972**, *1*, 12.

(8) Sakurai, H.; Sato, S.; Urabe, K.; Izumi, Y. *Chem. Lett.* **1985**, 1783.

(9) Delmastro, A.; Gozzelino, G.; Mazza, D.; Vallino, M.; Busca, G.; Lorenzelli, V. *J. Chem. Soc. Faraday Trans.* **1994**, *90*, 2663.

(10) Wang, W. J.; Che, Y. W. *Catal. Lett.* **1991**, *10*, 297.

(11) Peil, K.; Galya, L. G.; Marcelin, G. *J. Catal.* **1989**, *115*, 441.

(12) Engels, S.; Herold, E.; Lausch, H.; Mayr, H.; Meiners, H. W.; Wilde, M. *Proceedings of the 10th International Congress on Catalysis*, Budapest, Hungary, 19-24 July **1992**, 2581.

(13) Murakami, Y.; Otsuka, K.; Wada, Y.; Morikawa, A. *Bull. Chem. Soc. Jpn.* **1990**, *63 n°2*, 340.

(14) Cucinieri-Colorio, G.; Auroux, A.; Bonnetot, B. *J. Therm. Anal.* **1993**, *40*, 1267.

(15) Cucinieri-Colorio, G.; Bonnetot, B.; Védrine, J. C.; Auroux, A. *New Developments in Selective Oxidation II;* ed. V. Cortés Corberán and S. Vic. Bellón, Elsevier Science Publishers, 1994, 143.

(16) Colorio, G.; Védrine, J. C. ; Auroux, A. ; Bonnetot, B., *Appl. Catal. A: Gen.* **1996**, *137*, 55.

(17) Buyevskaya, O. V.; Kubik, M.; Baerns, M. *Symposium on Heterogeneous Hydrocarbon Oxidation Presented before the Division of Petroleum Chemistry, Inc., 211th National Meeting;* American Chemical Society: New Orleans, L.A., 24-29 March 1996, 163.

(18) Pine, L. *U.S. Patent* 3993557, 1976.

(19) Bailey, W. A. *US Patent* 2377744, 1945.

(20) De Bataafsche, N.V.; Petroleum Maatschappij, te's-Gravenhage, *Dutch Patent* 62287, 1949.

(21) De Bataafsche, N.V.; Petroleum Maatschappij, te's-Gravenhage, *Dutch Patent* 65287, 1950.

(22) Sato, S.; Kuroki, M.; Sodesawa, T.; Nozaki, F.; Maciel, G. E. *J. Mol. Cat. A: Chem.*, **1995**, *104*, 171.

(23) Izumi, Y.; Shiba, T. *Bull. Chem. Soc. Jpn.* **1964**, *37 n°12*, 1797.

(24) Tanabe, K. *Solid Acids and Bases, their catalytic properties*; Academic Press: New-York-London, 1970, 131.

(25) Xiaoding, X.; Boelhouwer, C.; Benecke, J. I.; Vonk, D.; Mol, J. C. *J. Chem. Soc. Faraday Trans. 1*, **1986**, *82*, 1945.

(26) Sibeijn, M.; van Veen, J. A. R.; Bliek, A.; Moulijn, J. A. *J. Catal.* **1994**, *145*, 416.

(27) Chen, Y. W.; Li, C. *Catal. Lett.* **1992**, *13*, 359.

(28) Nadirov, N. K.; Vozdvizhenskii, V. F.; Kondratkova, N. I.; Fatkulina, A. A. *React. Kinet. Catal. Lett.* **1985**, *27 (1)*, 191.

(29) Peil, K. P.; Galya, L. G.; Marcelin, G. *Catalysis: Theory to Practice*; 9th International Congress on Catalysis: Canada, 1988, 1712.

(30) Okihara, T.; Tamura, H.; Misono, M. *J. Catal.* **1995**, *95*, 41.

(31) de Rosset, A. J. *US Patent* 2938001, 1960.

(32) O'Hara, M. J. *US Patent* 3453219, 1969.

(33) Plundo, R. A. *US Patent* 3617532, 1971.

(34) Dufresne, P.; Marcilly, C. *French Patent* 2561945, 1985.

(35) Pine, L. A. *US Patent* 3954670, 1976.

(36) O'Hara, M. J. *US Patent* 3525684, 1970.

(37) O'Hara, M. J. *US Patent* 3666685, 1972.

(38) Polard, R. J.; Voorhies J. D. *US Patent* 4139492, 1979.

(39) Toulhoat, H. *European Patent* 0297949, 1989.

(40) Morishige, H.; Akai, Y. *Bull. Soc. Chim. Belg.* **1995**, *104 (4-5)*, 253.

(41) Stranick, M. A.; Houalla, M.; Hercules, D. M. *J. Catal.* **1987**, *104*, 396.

(42) Houalla, M.; Delmon, B. *Appl. Catal.* **1981**, *1*, 285.

(43) Vorob'ev, V. N.; Agzamkhodzhaeva, D. R.; Mikita, V. P.; Abidove, M. F. *Kinetika i Kataliz* **1984**, *25*, 154.

(44) Ramírez, J.; Castillo, P.; Cedeño, L.; Cuevas, R.; Castillo, M.; Palacios, J. M.; López-Agudo, A. *Appl. Catal. A: Gen.* **1995**, *132*, 317.

(45) Li, C.; Chen, Y. W.; Yang, S. J.; Wu, J. C. *Ind. Eng. Chem. Res.* **1993**, *32*, 1573.

(46) Tsai, M. C.; Chen, Y. W.; Kang, B. C.; Wu, J. C.; Leu, L. J. *Ind. Eng. Chem. Res.* **1991**, *30*, 1801.

(47) Chen, Y. M.; Tsai, M. C.; Kang, B. C.; Wu, J. C. *AIChE Summer National Meeting*, 1990, 101.

(48) Dubois, J. L.; Fujieda, S. *Catal. Today* **1996**, *29*, 191.

(49) Muralidhar, G.; Massoth, F. E.; Shabtai, J. *J. Catal.* **1984**, *85*, 44.

(50) Li, D.; Sato, T.; Imamura, M.; Shimada, H.; Nishijima, A. *J. Catal.* **1997**, *170*, 357.

(51) Lafitau, H.; Neel, E.; Clement, J. C. *Preparation of Catalysts*; ed. B. Delmon, P. A. Jabobs and J. Poncelet, Elsevier Scientific Publishing Company: Amsterdam, 1976, 393.

(52) Mertens, F. P.; Dai, E. P.; Bartley, B. H.; Neff, L. D. *Symposium on Advances in Hydrotreating Catalysts Presented before the Division of Petroleum Chemistry Inc., 208th National Meeting;* American Chemical Society: Washington D. C., August 1994, 1-26, 566.

(53) Dumeignil, F.; Guelton, M.; Rigole, M.; Amoureux, J. P.; Fernandez, C.; Grimblot, J. *J. Colloids Surf. A* **1998**, *158(1)*, 75.

(54) Dumeignil, F.; Guelton, M.; Rigole, M.; Grimblot, J. submitted to *Chem. Mater.* **2004**.

(55) Le Bihan, L.; Mauchaussé, C.; Duhamel, L.; Grimblot, J. *J. Sol-Gel Sci. Technol.* **1994**, *2*, 837.

(56) Kurokawa, Y.; Kobayahi, Y.; Nakata, S. *Heterogeneous Chem. Rev.* **1994**, *1*, 309.

(57) Tsuchida, T.; Ohta, S.; Horigome, K. *J. Mater. Chem.* **1994**, *4(9)*, 1503.

(58) Turner, G. L.; Smith, K. A.; Kirkpatrick, R. J.; Oldfield, E. *J. Magn. Reson.* **1986**, *67*, 544.

(59) Bray, P. J.; Edward, J. O.; O'Keefe, J. G.; Ross, V. F.; Tatsuzaki, I. *J. Chem. Phys.* **1961**, *35*, 435.

(60) Kriz, H. J.; Bishop, S. B.; Bray, P. J. *J. Chem. Phys.* **1968**, *49*, 557.

(61) Lai, K. C.; Petch, H. E. *J. Chem. Phys.* **1965**, *43(1)*, 178.

(62) Scholle, K. F. M. G. J.; Veeman, W. S. *Zeolites* **1985**, *5*,118.

(63) Zhong, J.; Bray, P. J. *J. Non-cryst. Solids* **1989**, *11*, 67.

(64) Sato, S.; Kuroki, M.; Sodesawa, T.; Nozaki, F.; Maciel, G. E. *J. Mol. Cat. A: Chem.* **1995**, *104*, 171.

(65) Peil, K. P.; Galya, L. G.; Marcelin, G. *J. Catal.* **1989**, *115*, 441.

(66) Dubois, J. L.; Fujieda, S. *Preparation of Catalysts VI, Scientific bases for the Preparation of Heterogeneous Catalysts*; ed. G. Poncelet *et al.*, 1995, 833.

(67) Amoureux, J. P.; Fernandez, C.; Carpentier, L.; Cochon, E. *Phys. Stat. Sol. (a)* **1992**, *132*, 461.